

Palladium Nanoparticles Supported on Mesoporous Silica as Efficient and Recyclable Heterogeneous Nanocatalysts for the Suzuki C–C Coupling Reaction

Phendukani Ncube¹ · Thaane Hlabathe¹ · Reinout Meijboom¹

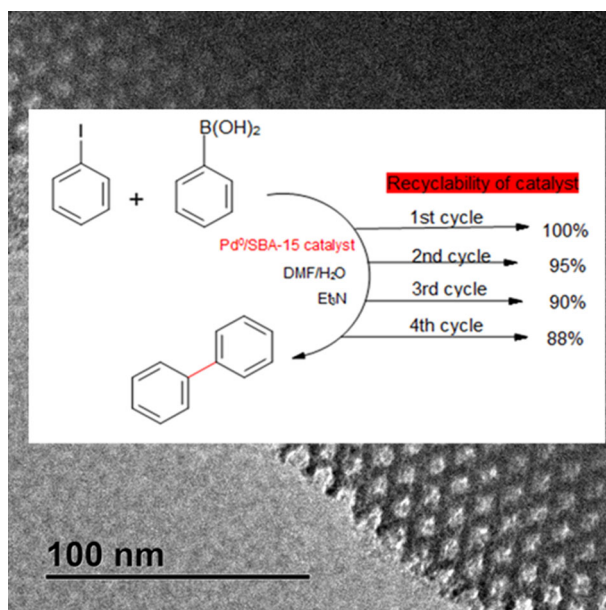
Received: 3 March 2015 / Published online: 6 May 2015
© Springer Science+Business Media New York 2015

Abstract Palladium (Pd) nanoparticles were synthesized using the dendrimer-tem-plate method and then immobilized on a silica support (SBA-15). The SBA-15 support material was specifically synthesized with a pore size large enough ($d = 6.6$ nm) to accommodate the dendrimer generation used (G-5 PAMAM-OH; $d = 5.4$ nm). The morphology of the Pd-supported catalyst (Pd⁰/SBA-15) was characterized by scanning electron microscopy coupled to an energy dispersive X-ray spectrometer which confirmed the elemental composition of the catalyst. Transmission electron microscopy confirmed the ordered array of the mesoporous SBA-15 and showed that the Pd NPs were indeed immobilized inside the pores. The catalyst had a pore size of 5.7 nm, a pore volume of 0.78 cm³/g and a surface area of 493 m²/g as determined by surface adsorption/desorption measurements from BET analysis. The prepared Pd⁰/SBA-15 catalyst was an efficient recyclable heterogeneous catalyst for Suzuki coupling. The catalytic activity was investigated using different experimental conditions such as temperature, catalyst loading, base and solvent variations. The catalyst gave high conversions and turnover frequencies even in aqueous solutions and at fairly low temperatures showing the potential for the green synthesis of important organic molecules through C–C bond formation.

✉ Reinout Meijboom
rmeijboom@uj.ac.za

¹ Department of Chemistry, Research Centre for Synthesis and Catalysis, University of Johannesburg, P O Box 524, Auckland Park, Johannesburg 2006, South Africa

Graphical Abstract



Keywords Palladium nanoparticles · SBA-15 · Catalysis · Suzuki C–C coupling

Introduction

Metal nanoparticles have attracted much interest in scientific research and industrial application due to their large surface area [1–3]. Industrial catalysts are normally composed of inorganic supports such as silica and titania to overcome the environmental problems that might be caused by some of the hazardous metals, such as being lethal to the species which survive in water. Most of the waste from the industries is being discharged to the rivers and dams. Small molecule solid phase synthesis has become a great tool in the discovery of new drugs and molecular materials. The following reactions are used in the synthesis of important organic molecules and these molecules are highly important in the synthesis of pharmaceuticals which are important to the health issues and in many other applications in life.

Palladium catalyzed C–C coupling reactions have received great attention worldwide as shown by several extensive reviews [4–9]. The reactions include the Suzuki cross coupling of aryl halides with aryl boronic acids [10–22], the Heck reaction between an aryl or alkyl halide and a vinyl functionality [23–27], the Sonogashira reaction [28–30], and the cross coupling reaction of organostannyl reagents with a variety of organic electrophiles named the Stille reaction [30]. Although homogeneous palladium catalysts have been extensively investigated [31–36], their industrial applications remain limited due to the difficulty in the separation

process from the products for recycling [37–40]. Heterogenization of the existing homogeneous palladium catalysts, therefore, offers an attractive solution to this problem.

In this study, we report on the preparation of palladium nanoparticles supported on SBA-15 mesoporous material without the need for prior functionalization of the silica support. We use the dendrimer template method for the synthesis of the nanoparticles and then match the diameter of the dendrimer generation to the pore size of the mesoporous SBA-15. In this way the NPs are efficiently immobilized inside the pores of the support and subsequent calcination removes the organic dendrimer, leaving NPs well dispersed inside the pores of the SBA-15. The prepared catalyst was then used to catalyse the Suzuki C–C bond formation reaction between phenyl boronic acid and aryl halides. The influence of different reaction conditions including temperature, base, catalyst loading and type of aryl halide are reported. The use of water as a solvent for the coupling reaction is also explored as an approach towards a greener method of organic synthesis.

Experimental

Materials and Equipment

Generation five hydroxyl-terminated poly (amido)amine (G-5 PAMAM-OH; 5 wt% in MeOH) dendrimers, potassium tetrachloropalladate(II) (K_2PdCl_4), sodium borohydride ($NaBH_4$), phenylboronic acid, iodobenzene (PhI), bromobenzene (PhBr), chlorobenzene (PhCl), tetraethyl orthosilicate (TEOS), pluronic P123 ($EO_{20}PO_{70}EO_{20}$) and triethylamine (Et_3N) were all purchased from Sigma-Aldrich. Sodium carbonate (Na_2CO_3), sodium hydrogen carbonate ($NaHCO_3$) and sodium acetate ($NaOOCCH_3$) were purchased from Merck Chemicals. The methanol in the dendrimer solutions was removed in vacuo before use while all other chemicals were used without further purification. All solutions were prepared in Milli-Q (18.3 M Ω -cm) water. Scanning electron micrographs were taken on a Tescan Vega 3LMH scanning electron microscope with the samples carbon-coated on copper grids using an Agar Turbo Carbon Coater. High resolution transmission electron microscopy (HRTEM) was performed on a JEOL JEM-2100F electron microscope with an accelerating voltage of 200 kV. Nitrogen adsorption/desorption measurements were performed on a Micromeritics TriStar 2460 surface area and porosity analyzer with a Micromeritics Degas System for degassing samples prior to analysis. Thermogravimetric analysis (TGA) was performed on an SDT Q600 Thermogravimetric Analyzer while infra-red spectra were taken using a Bruker Tensor 27 Fourier transform infrared spectrometer. Gas chromatographic measurements were performed on a Shimadzu GC-2010 Plus while mass spectra were taken on a Shimadzu GCMS-QP2010. Metal loadings were determined using a Spectro Arcos FSH12 Inductively-coupled plasma optical emission (ICP-OES) spectrometer.

Preparation of Catalyst

Synthesis of SBA-15 Support

The mesoporous support was synthesized using the surfactant method reported by Zhao et al. [41, 42] and later modified by Vunain et al. [43]. Briefly, the surfactant tri-block copolymer pluronic P123 (EO₂₀PO₇₀EO₂₀) (8.250 g) was dissolved in deionized water (40 mL) by stirring at room temperature for 30 min. After all the surfactant had dissolved, HCl (2 M, 360 mL) was added and the solution stirred in an oil bath pre-heated to 40 °C for a further hour. After 1 h, tetraethyl orthosilicate (18.0 mL) was added and the mixture stirred at 40 °C for 24 h. The temperature was then raised to 90 °C and the white slurry formed aged without stirring for 48 h. The reaction was then cooled to room temperature and then the white product collected by vacuum filtration. The solid was washed with copious amounts of water and then dried at 100 °C in an oven. The resulting powder was heated at a rate of 1.0 °C/min to 550 °C for 8 h and then calcined at 550 °C for 4 h. The oven was allowed to cool to room temperature.

Synthesis of Pd⁰/SBA-15 Catalyst

To a stirred aqueous solution of G-5 PAMAM dendrimer (2.5×10^{-3} M; 100 μ L), an aqueous solution of K₂PdCl₄ (0.1 M; 200 μ L) was added to give a Pd²⁺/dendrimer ratio of 80. The solution was stirred for 1 h under a N₂ atmosphere to allow coordination of Pd²⁺ ions to the interior amines of the dendrimer. This was followed by the addition of a tenfold equivalent of NaBH₄ solution (1.0 M; 200 μ L) with continued stirring. The solution immediately turned brown due to the formation of Pd dendrimer-encapsulated nanoparticles (PdDENs). The PdDENs formed were characterized by UV/Vis spectrophotometry as well as TEM prior to the addition of SBA-15 support. To the solution of the pre-formed PdDENs was then added 1.0 g of the previously synthesized SBA-15 and the heterogeneous mixture stirred for 16 h at ambient temperature. The solid catalyst was collected by centrifugation on a Hettich Universal centrifuge set at 100 % and a speed of 4000 rpm for 1 h. The grey solid was then dried at 100 °C and part of the sample was then calcined at 550 °C to remove the dendrimer template.

General Experimental Procedure for Suzuki C–C Coupling Reaction

The coupling of phenylboronic acid, PhB(OH)₂ with aryl halides (Ph-I, Ph-Br and Ph-Cl) was carried out under various conditions. In a typical reaction, the boronic acid (1.2 mmol), aryl halide (1.0 mmol), base (2.0 mmol) and the nanocatalysts were stirred in a solvent (10 mL) in a 25 mL two-necked round-bottomed flask. The reaction was carried out at various temperatures and various catalyst loadings. Stirring was stopped at time intervals and samples taken and filtered using a syringe filter (0.22 μ m pore size). The filtered samples (100.0 μ L) were then diluted to 1.0 mL and analyzed by GC. Confirmation of products was done by the use of certified standards as well as by GC–MS.

Results and Discussion

Preparation and Characterization of Catalyst

The DENs were characterized prior to immobilization on the silica support using UV/Vis spectrophotometry, FT-IR and HRTEM. From the UV–Vis spectrophotometric analysis the formation of metal nanoparticles was confirmed. In Fig. 1a, a band at λ 208 nm appears after the addition of Pd^{2+} to the dendrimer solution due to ligand-to-metal charge transfer (LMCT) which corresponds to the complexation of Pd^{2+} ions to the tertiary amines of the dendrimer interior [44]. The addition of reducing agent results in the disappearance of the LMCT band confirming the reduction of Pd^{2+} to zerovalent Pd. The size and size distribution of the PdDENs was determined by HRTEM (Fig. 1b) and the corresponding size distribution histogram is shown in Fig. 1c. The average diameters measured were obtained by counting 250 nanoparticles from several TEM images and the average diameter of the PdDENs was found to be 2.14 ± 0.35 nm.

The pore diameters (5.4 and 5.7 nm), BET surface areas (S_{BET}) (813.8 and 493.6 m^2/g) and the total pore volumes (0.85 and 0.78 cm^3/g) of the calcined SBA-15 support as well as the $\text{Pd}^0/\text{SBA-15}$ catalyst respectively, were determined from BET analysis. The pore diameter, a high surface area and pore volume obtained for the calcined support are all consistent with the values obtained using similar synthetic methods for SBA-15 [43, 45]. There was a significant decrease in the surface area after the immobilization of the Pd nanoparticles. The N_2 adsorption–desorption isotherms (Fig. 2a) showed that the isotherms were of Type IV with a H1 hysteresis loop, typical of mesoporous materials with ordered pore structures, as classified by the International Union of Pure and Applied Chemistry (IUPAC) [46]. The plot of pore volume per unit length versus the pore diameter for the SBA-15 support and for the $\text{Pd}^0/\text{SBA-15}$ catalyst is shown in Fig. 2b. The fact that both the

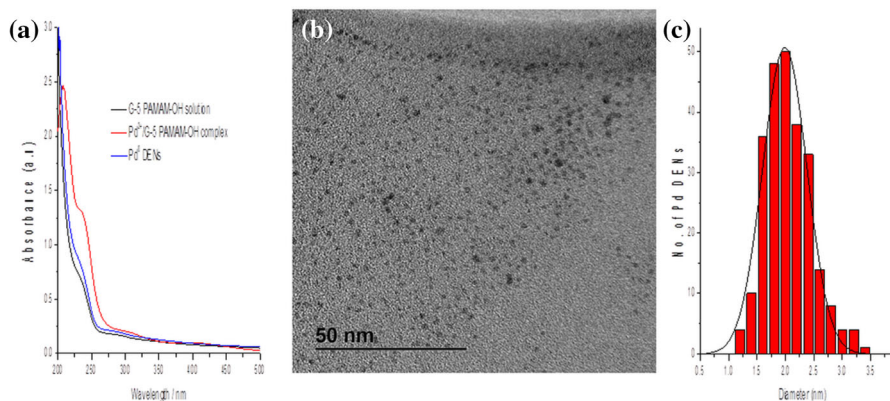


Fig. 1 Characterization of PdDENs; **a** UV/Vis spectrophotometry, **b** HRTEM image of PdDENs and **c** the size distribution histogram of the PdDENs

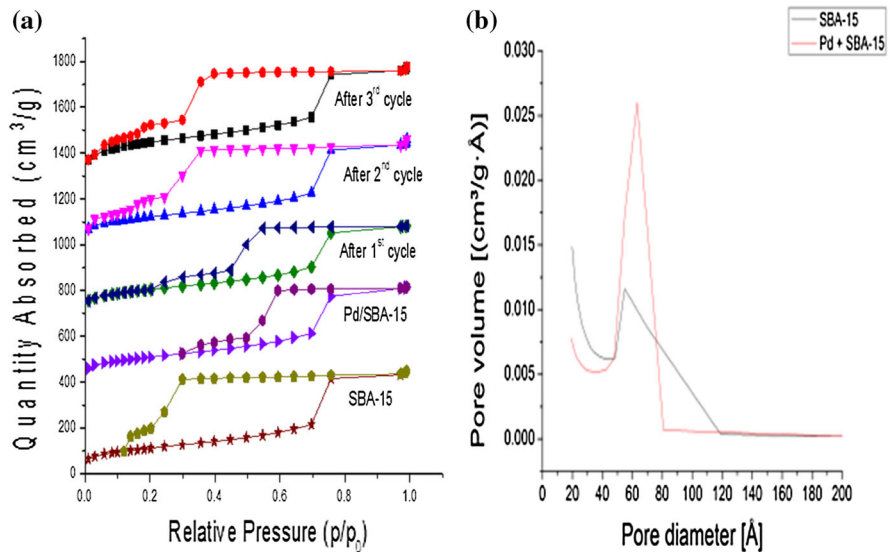


Fig. 2 **a** N_2 -adsorption/desorption isotherms for as synthesized SBA-15 and Pd/SBA-15 catalyst for three consecutive cycles and the pore diameter of SBA-15 and Pd/SBA-15 and **b** plot of pore diameter against pore volume

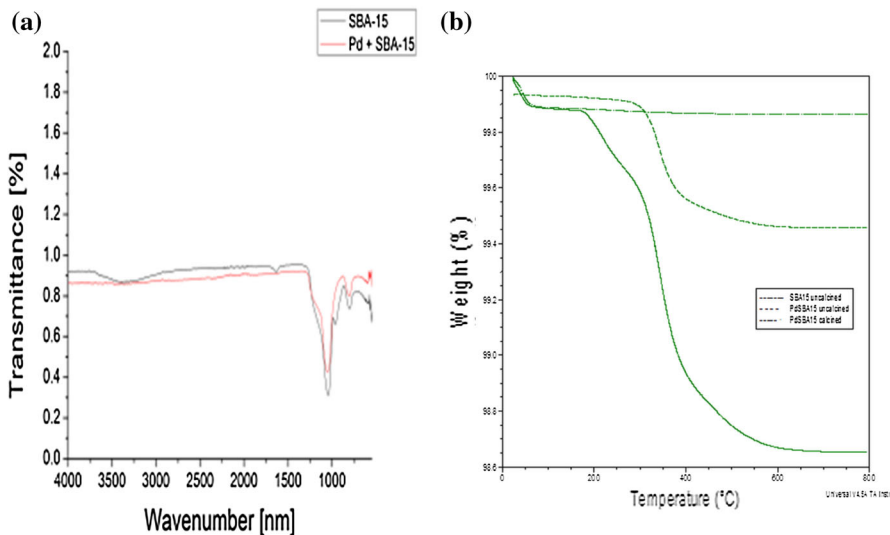


Fig. 3 **a** FTIR spectra and **b** TGA thermo-grams of SBA-15 and Pd-SBA-15 catalyst

pore size and surface area decreased upon the introduction of Pd is good evidence that the metal nanoparticles were deposited primarily inside the mesopores of the SBA-15.

The FTIR spectra of the SBA-15 and Pd-SBA-15 are depicted in Fig. 3a. The characteristic absorption band for SBA-15 is present at ν 3384 cm^{-1} and it shows the presence of Si-OH groups, which is not present after SBA-15, is being loaded with palladium. The asymmetric stretch of Si-O-Si bonds was observed at ν 1044 cm^{-1} for SBA-15 and at ν 1050 cm^{-1} for Pd-SBA-15. In SBA-15 there is a weak peak at ν 962 cm^{-1} which is absent in Pd-SBA-15. Similar results were reported by Ivashchenko et al. [47] The thermo-gravimetric traces of the SBA-15 and Pd/SBA-15 in Fig. 3b show a very small initial weight loss (0.1 %) below 100 °C which shows that the materials does not absorb large amounts of moisture from the air. The overall weight loss of about 1.4 %, observed for un-calcined Pd⁰SBA-15, was due to the loss of the dendrimer template while only a loss of 0.5 % for the calcined catalysts was observed proving that the stability of the material is very suitable for high temperatures as is one of the requirements for heterogeneous catalysis. These results showed that our catalyst was both air and thermally stable, meaning that it can therefore be used at ambient atmosphere and is stable up to high temperatures.

A typical SEM image of the Pd⁰/SBA-15 catalyst shown in Fig. 4a show that the morphology of our catalyst consist of well-defined surface of rod-shaped particles, similar to that obtained by Veisi et al. [12] as well as Alizadeh and co-workers [20]. The presence of metallic Pd in the catalyst was confirmed by EDX analysis (Fig. 4b), which also clearly showed the Si and O from the SBA-15 support. The peaks observed from C were due to the carbon-coating used in preparing the sample, while a small amount of residual Na was from the NaBH₄ used as reducing agent in the formation of the nanoparticles. Transmission electron micrographs (Fig. 5a) show the ordered pore array in the synthesized matrices as well as the honey-comb porous structure characteristic of SBA-15 materials [48]. HRTEM micrographs

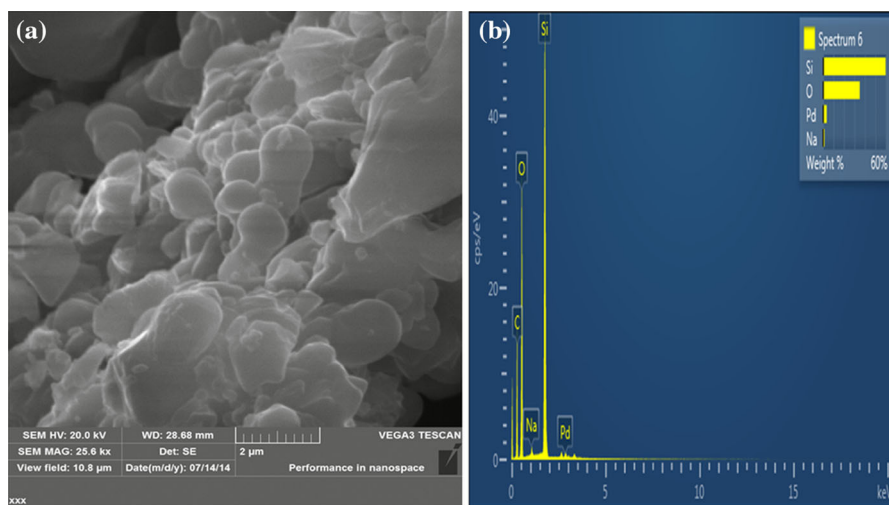


Fig. 4 a Scanning electron micrograph of Pd⁰/SBA-15 catalyst and b EDX spectrum showing elemental composition of the catalyst

showing the supported Pd NPs (Fig. 5b, c) show clearly that the nanoparticles are inside the pore channels of the SBA-15 support and that introduction of the metal do not alter the ordered matrix of the support. Even though it was difficult to get a statistical number of clearly visible supported nanoparticles due to the support matrix, it was clear from a sample such as in Fig. 5c that there was no significant agglomeration of the Pd DENs upon immobilization on the SBA-15 support.

The small angle X-ray diffraction (XRD) patterns of SBA-15 and Pd⁰/SBA-15 catalyst (Fig. 6a) show a typical three-peak pattern with a strong diffraction and two small diffraction peaks for the 100, 110 and 200 planes confirming a well-defined hexagonal symmetry and long-range ordering of structure [12, 47, 48]. The similar pattern for the SBA-15 and the catalysts indicate that the method used for the immobilization of the Pd nanoparticles does not alter the ordered structure of the

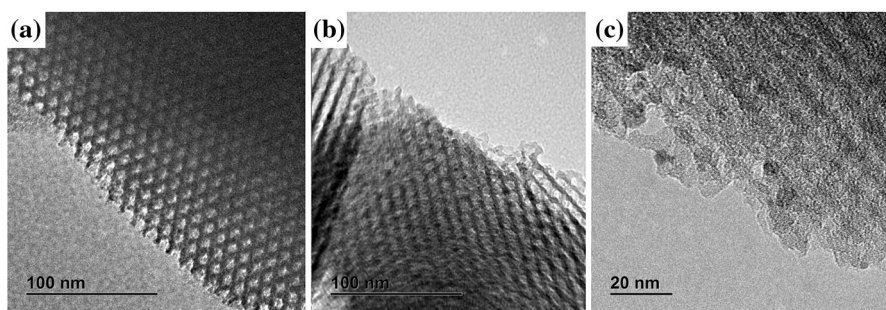


Fig. 5 HRTEM micrographs of **a** SBA-15, **b** Pd⁰/SBA-15 catalyst and **c** a magnified portion of Pd⁰/SBA-15 catalyst showing Pd⁰ NPs on the support mesopores

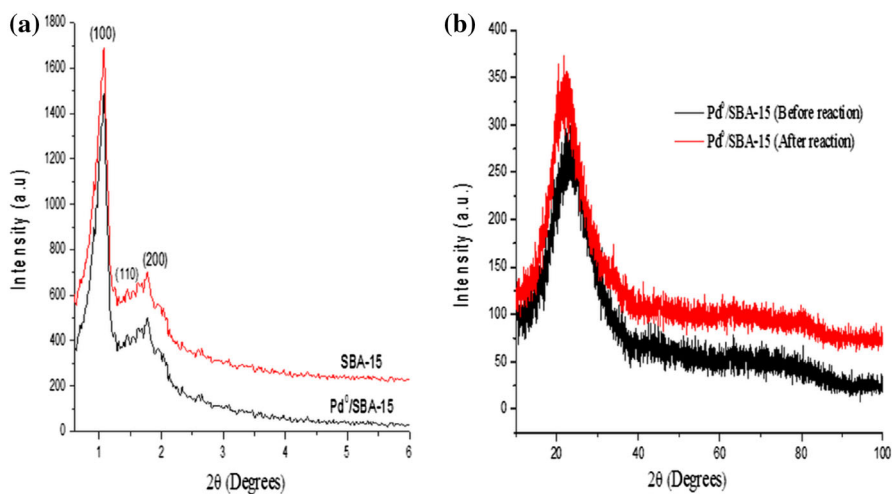


Fig. 6 **a** Low-angle powder X-ray diffraction spectra for the as synthesized SBA-15 support and the Pd⁰/SBA-15 catalyst and **b** high-angle X-ray diffraction spectra of the catalysts before and after four cycles of reaction

support. Due to the very small metal loadings used in preparing our catalyst, high angle XRD (Fig. 6b) showed no peaks for the Pd in the catalyst, but the spectra is shown here for comparison before and the catalytic reaction showing the stability of our catalyst. The TEM and p-XRD confirmed that no large particles were present in the catalyst and that all Pd nanoparticles were less than 10 nm in diameter.

Catalytic Activity

There is a need to have easily prepared and recyclable heterogeneous catalysts for reactions that are important in producing fine chemicals such as C–C coupling reactions. Different parameters that have previously [49, 50] been shown to affect the Suzuki coupling, namely; catalyst loading, solvent, base and the type of aryl halide substrate were investigated. To optimize reaction conditions iodobenzene and phenylboronic acid were used as model substrates. Iodobenzene was then replaced by different aryl halides to investigate the effect of changing the substrate. The effect of varying temperature on the reaction was also done and the thermodynamic parameters calculated from the results of the temperature variations.

Influence of Metal Loading

The influence of the amount of Pd metal in the catalyst was determined for the reaction between iodobenzene and phenylboronic acid at 110 °C in DMF/H₂O with Et₃N as the base. Increasing the amount of Pd resulted in an increase in the percentage conversion of PhI into biphenyl (Fig. 7). The reaction had reached conversions greater than 90 % within an hour for the metal loading of 0.05 mol% Pd while the lowest metal loading (0.015 %) gave only about 20 % conversion even after 7 h reaction time. The rate constants for the different catalyst loadings were

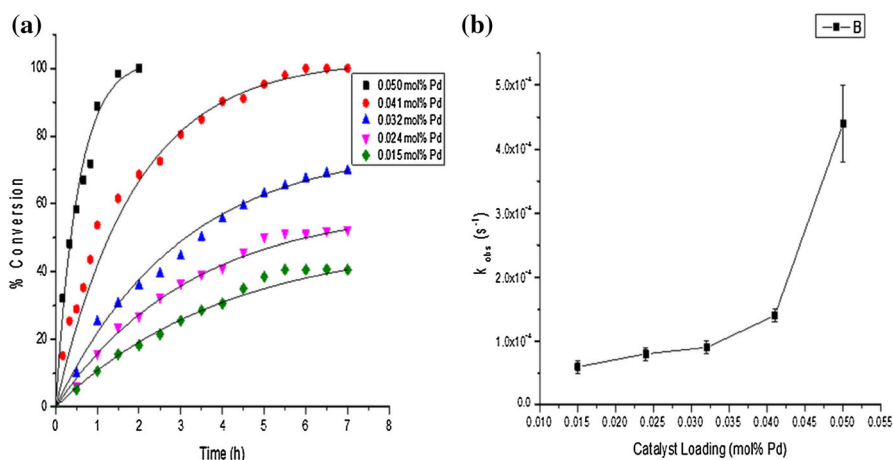


Fig. 7 **a** Influence of catalyst amount on the conversion of iodobenzene and **b** rate constants as a function of catalyst amount

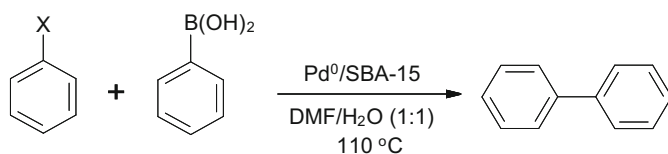
calculated using the Kinetic studio software (Tgk Scientific Limited version 2.08; 2010) and as expected values increased with increasing amount of catalyst showing that the reaction was indeed a catalytic reaction, catalyzed by our prepared Pd⁰/SBA-15 catalyst. The highest metal loading of 0.05 mol% Pd was used for optimizing other reaction conditions.

Influence of Base and Different Solvents

We investigated the influence of using different solvents on the Suzuki coupling between iodobenzene and phenylboronic acid. The catalyst loading was maintained at 0.05 mol% Pd. Different bases were also employed to see their influence on the reaction. We first used five solvent systems with the same base Et₃N (Table 1 entries 1–5). DMF gave the best TOF of 1996 h⁻¹ (entry 1) while an attempt to use water as the solvent gave poor yield in 1 h and only 15.1 % after 5 h (TOF = 60.4 h⁻¹). However a significant improvement in the reaction was observed when we used water in combination with DMF resulting in a yield of 98.5 % (TOF = 1313.3 h⁻¹) albeit in a slightly longer reaction time of one and half hours (entry 3). The use the alcohols MeOH (entry 4; TOF = 468.6 h⁻¹) and EtOH (entry 5; TOF = 453.3 h⁻¹) gave moderate performance with yields around 70 % after 3 h reaction time. We therefore did not further explore these solvents, instead focused on the more interesting DMF and water solvent systems by investigating the effect of using different bases. For DMF as the solvent we observed that changing from the organic base (Et₃N) to the inorganic bases (Na₂CO₃, NaHCO₃ and CH₃COONa) there was significant drop in reaction activity, with TOF values dropping from 1996 h⁻¹ for Et₃N (entry 1) to 164.4 h⁻¹ for CH₃COONa (entry 8). Poor activity was also observed when pyridine was used as a base (entry 9, TOF = 20 h⁻¹). A possible explanation for the poor catalytic activity when using the inorganic bases is the poor miscibility with the solvent DMF. In this light we therefore explored the use of these inorganic bases with water only as the solvent. Only NaHCO₃ and CH₃COONa (entries 10 and 11) were used and we observed that reaction activity was indeed improved from a TOF = 60.4 h⁻¹ Et₃N (entry 2) to TOF values of 160 and 124 h⁻¹ for NaHCO₃ and CH₃COONa respectively. We also investigated the 1:1 DMF/H₂O solvent system using different bases. We observed that using this solvent system gave similar activity with all the bases with TOF values of 1313.3, 1310.7 and 1042.7 h⁻¹ for Et₃N, NaHCO₃ and CH₃COONa respectively (entries 3, 12 and 13 in Table 1).

Influence of Varying Aryl Halide Substrate

We also investigated the influence of using different aryl halide substrates. The measured conversions after an hour are shown in Table 2. The cross-coupling reaction was seen to decrease in the order I > Br > Cl as the halide group and using DMF as solvent (entries 1–3 in Table 2). This trend can be explained by the decrease in bond energy in the order C–I < C–Br < C–Cl which makes it increasingly difficult to activate the C–X bond for the oxidative addition of Pd to form C–Pd–X catalyst species which is suggested in the mechanism for Pd catalyzed C–C coupling reactions [51]. We further explored the use of substituted

Table 1 The influence of using different solvents and bases on the Suzuki C–C coupling reaction

Entry	Solvent	Base	Time (h)	Yield (%) ^a	TOF (h ⁻¹)
1	DMF	NEt ₃	1	99.8	1996
2	H ₂ O	NEt ₃	5	15.1	60.4
3	DMF:H ₂ O (1:1)	NEt ₃	1.5	98.5	1313.3
4	MeOH	NEt ₃	3	70.3	468.6
5	EtOH	NEt ₃	3	68.0	453.3
6	DMF	Na ₂ CO ₃	5	49.8	199.2
7	DMF	NaHCO ₃	5	54.1	216.4
8	DMF	CH ₃ COONa	5	41.1	164.4
9	DMF	Pyridine	5	5.0	20.0
10	H ₂ O	NaHCO ₃	5	40.0	160.0
11	H ₂ O	CH ₃ OONa	5	31.0	124.0
12	DMF:H ₂ O (1:1)	NaHCO ₃	1.5	98.3	1310.7
13	DMF:H ₂ O (1:1)	CH ₃ OONa	1.5	78.2	1042.7

Reaction conditions: iodobenzene (1 mmol), phenylboronic acid (1.2 mmol), base (2 mmol), solvent (10 mL), 110 °C, catalyst loading = 0.05 mol% Pd

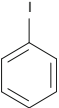
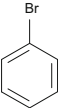
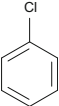
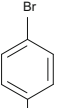
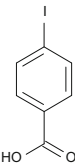
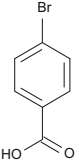
^a Yields were determined by GC-FID

aryl halides as substrates in the Suzuki coupling (entries 4–6). We observed that having a methyl group on the bromobenzene substrate (entry 4 in Table 2) only slightly increased the activity from a TOF of 802 h⁻¹ for bromobenzene (entry 2 in Table 3) to a TOF of 906 h⁻¹ for 4-methyl bromobenzene (entry 4 in Table 2) when using DMF as solvent. A decreased activity was however observed with the introduction of water in the solvent system and we therefore did not further explore the influence of any other alkyl substituted aryl benzenes. We investigated two carboxylic acid substituted aryl benzenes (entries 5 and 6 in Table 2). We observed that these gave high activity even in water both of which are comparable with that for iodobenzene in DMF (entry 1). This is important as the use of water as a solvent means biphenyl compounds with water miscible substituents can be synthesized under Green conditions.

Influence of Temperature: Determination of Thermodynamic Parameters

The reaction was carried out at four different temperatures (353, 363, 373 and 383 K). The time course of the reaction at the four temperatures used is shown in Fig. 8a and the rate constants (k_{obs}) of $2.15 (\pm 0.11) \times 10^{-4} \text{ s}^{-1}$; $2.93 (\pm 0.19) \times 10^{-4} \text{ s}^{-1}$; $4.65 (\pm 0.16) \times 10^{-4} \text{ s}^{-1}$ and $7.77 (\pm 0.16) \times 10^{-4} \text{ s}^{-1}$ for

Table 2 The influence of varying aryl halide substrate on the Suzuki C–C coupling reaction

Entry	Aryl halide	Solvent	Yield (%) ^a	TOF (h ⁻¹)
1		DMF	99.8	1996
		DMF/H ₂ O (1:1)	94.3	1886
2		DMF	40.1	802
		DMF/H ₂ O (1:1)	28.5	570
3		DMF	15.0	300
		DMF/H ₂ O (1:1)	10.6	212
4		DMF	45.3	906
		DMF/H ₂ O (1:1)	25.2	504
5		DMF/H ₂ O (1:1)	98.8	1976
		H ₂ O	99.5	1990
6		DMF/H ₂ O (1:1)	78.6	1572
		H ₂ O	90.5	1810

Reaction conditions: iodobenzene (1 mmol), phenylboronic acid (1.2 mmol), base (2 mmol), solvent (10 mL), 110 °C, catalyst loading = 0.05 mol% Pd, reaction time = 1 h

^a Yields were determined by GC-FID

the four temperatures respectively, thus obtained are plotted against temperature in Fig. 8b. Figure 8b shows the typical exponential increase of the rate constants as the temperature increases. From the temperature variation experiments, the activation energy ($E_A = 48.32 \text{ kJ mol}^{-1}$) for the reaction was calculated using the Arrhenius equation (Eq. 1), while the enthalpy change ($\Delta H = 45.27 \text{ kJ mol}^{-1}$) and entropy change ($\Delta S = -43.03 \text{ J mol}^{-1}$) were calculated using the Eyring equation (Eq. 2)

$$\ln(k_{obs}) = \ln A - \frac{E_A}{RT} \quad (1)$$

$$\ln\left(\frac{k_{obs}}{T}\right) = -\frac{\Delta H}{RT} + \ln\left(\frac{k_B}{h}\right) + \frac{\Delta S}{R}. \quad (2)$$

Table 3 Comparison of catalytic activity of present catalyst with other Pd supported catalysts reported in literature

Catalyst	Aryl halide	Yield (%) (reaction time)	TOF (h ⁻¹)	Reference
Pd(II)/SBA-15	PhI	98 (0.2 h)	1633	[12]
	PhBr	98 (0.8 h)	408.3	
	PhCl	70 (10 h)	23.33	
Pd(II)/MCM-41	PhI	98 (1 h)	1735	[14]
	PhBr	100 (0.5 h)	2124	
	PhCl	85 (24 h)	63	
Pd ⁰ /montmorillonite	PhI	90 (1 h)	340.9	[19]
	PhBr	82 (5 h)	59.30	
	PhCl	82 (8 h)	40.20	
Pd/molecular organic framework	PhI	98 (1 h)	96.0	[15]
	(CHO)PhBr	94 (6 h)	78.3	
Pd ⁰ /SBA-15	PhI	99.8 (1 h)	1996	This work
	PhBr	80.2 (4 h)	802	
	PhCl	60.0 (4 h)	300	

Catalyst Leaching and Recyclability

Leaching of Catalyst: Hot Filtration Test

An important method commonly used to determine whether a catalyzed reaction is truly heterogeneous or not is the hot filtration test [14]. This method is used to rule out the possibility of homogenous or semi-heterogeneous catalysis. The test is carried out by running the reaction for a period of time and then filtering off the catalyst and allowing the reaction to proceed without the solid catalyst. No catalytic activity was observed with the filtrate, as shown by no increase in the product (determined by GC measurements). This confirmed that no Pd leached into solution and that our catalyst was acting as a heterogeneous catalyst in the performed C–C coupling reaction. To further confirm that no significant Pd metal had leached out of the support, ICP-OES was used to determine the amount of metal in the filtrate and again this gave negligible readings.

Recyclability of Catalyst

The reusability of catalysts is one of the most important benefits of heterogeneous catalytic systems from an economic point of view. The recyclability of our catalyst was investigated for the reaction between iodobenzene and phenylboronic acid by carrying out four consecutive cycles using the same reaction conditions. After each run, the catalyst was recovered by filtration, washed with acetone and water, then dried at 110 °C in an oven and subsequently used with fresh reactants. The catalytic activity did not change considerably after four cycles as shown in Fig. 9a. Evidence that the characteristics of the catalyst remain unchanged after the successive runs is

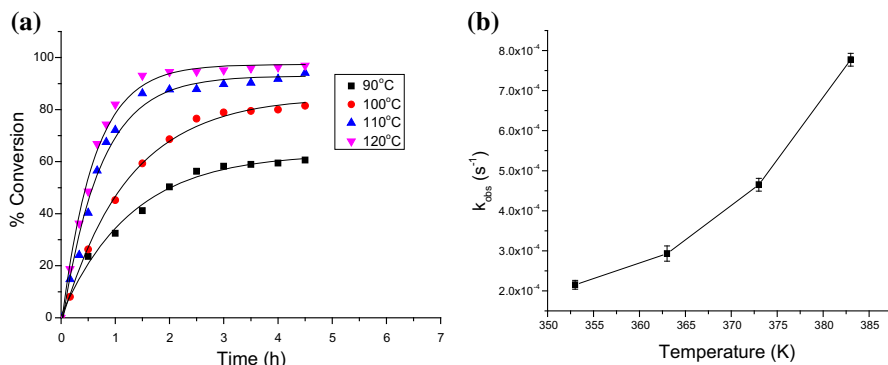


Fig. 8 **a** The effect of temperature on the conversion of iodobenzene (1 mmol) in the reaction with phenyl boronic acid (1.2 mmol) and Et₃N (2 mmol) as the base; **b** the observed rate constant as a function of temperature

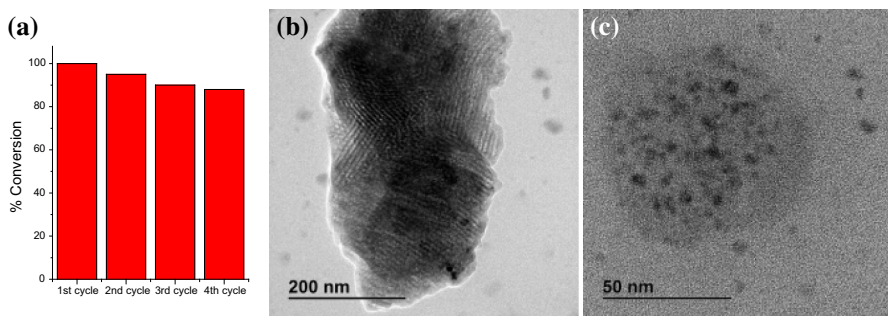


Fig. 9 **a** Recycling efficiency of Pd⁰/SBA-15 catalyst. **b** Low and **c** high magnification HRTEM micrographs of the catalyst after four cycles

shown by the identical shapes of the N₂-adsorption/desorption isotherms and the hysteresis loops of the recovered catalysts (Fig. 2). In addition, HRTEM images of the recovered catalyst after four cycles show that the ordered mesoporous structure of the SBA-15 support remains intact as seen in Fig. 9b and also there was no significant agglomeration of the Pd nanoparticle clusters which remained well-dispersed as shown in Fig. 9c.

Comparison with Other Supported Pd Catalysts

Several reports on the use of Pd-catalyzed cross-coupling reactions either as Pd⁰ or Pd(II) on solid supports have been reported in literature [7, 12, 14, 15, 19, 52]. Table 3 shows a comparison of the catalytic activity of our catalyst with other supported Pd catalysts. Our catalyst shows higher catalytic activity as shown by TOF values as well as comparable yields when compared to the other selected

systems. Moreover, our catalyst showed higher TOF's for the usually less reactive aryl chlorides (Table 3) and is, therefore, more applicable to a large variety of substituents.

Conclusion

In conclusion, silica-supported palladium nanocatalysts were prepared, characterized by various techniques and shown to be catalytically active towards the Suzuki C–C coupling reaction between aryl halides and phenyl boronic acid. The characterization of the catalyst using p-XRD and HRTEM showed that Pd nanoparticles of diameters less than 5 nm were immobilized inside the mesopores of the SBA-15 support. The catalyst was shown to be active depending on the type of base used as well as the type of aryl halide substrate used in the coupling reaction. The solvent also had an effect on the catalytic activity, while an increase in temperature resulted in increased conversions of the aryl halide in a short time as seen in by the determined observed rate constants (k_{obs}). The carboxylic acid substituted aryl halides were easily coupled to phenyl boronic acid in water due to their increased solubility as compared to the less miscible un-substituted counterparts which gave poor conversions in water. It was possible to recover the catalysts and re-use it while maintaining good catalytic activity up to four successive cycles. The ability to carry out the Suzuki coupling in water medium for some of the substrates and the recyclability of the catalyst shows that the reaction can be carried out under the desirable reaction conditions of Green Chemistry.

Acknowledgments This work is based on the research supported in part by the National Research Foundation of South Africa (Grant specific unique reference number (UID) 85386). We would also like to thank the University of Johannesburg for funding, Dr. Meyer and Mr. Harris of Shimadzu South Africa for the use of their instruments, Mrs. Tutuzwa, the HRTEM operator at CSIR.

References

1. G. Schmid *Clusters and Colloids. From Theory to Applications* (VCH, Weinheim, 1994).
2. Y. S. N. Toshima in A. T. Hubbard (ed.), *Encyclopedia of Surface and Colloid Science* (Marcel Dekker, New York, 2002).
3. N. Toshima and T. Yonezawa (1998). *N. J. Chem.* **22**, 1179.
4. N. Miyaura and A. Suzuki (1995). *Chem. Rev.* **95**, 2457.
5. C. Deraedt, D. Astruc (2013). *Accounts of Chemical Research.*
6. C. C. C. JohanssonSeechurn, M. O. Kitching, T. J. Colacot, and V. Snieckus (2012). *Angew. Chem. Int. Ed.* **51**, 5062.
7. L. Yin and J. Liebscher (2006). *Chem. Rev.* **107**, 133.
8. C. Tucker and J. de Vries (2002). *Top. Catal.* **19**, 111.
9. J. Durand, E. Teuma, and M. Gómez (2008). *Eur. J. Inorg. Chem.* **2008**, 3577.
10. N. Miyaura and A. Suzuki (1979). *J. Chem. Soc. Chem. Commun.* **19**, 866.
11. N. Miyaura, K. Yamada, and A. Suzuki (1979). *Tetrahedron Lett.* **20**, 3437.
12. H. Veisi, M. Hamelian, and S. Hemmati (2014). *J. Mol. Catal. A* **395**, 25.
13. A. Fodor, Z. Hell, and L. Pirault-Roy (2014). *Appl. Catal. A* **484**, 39.
14. S. Das, S. Bhunia, T. Maity, and S. Koner (2014). *J. Mol. Catal. A* **394**, 188.
15. A. S. Roy, J. Mondal, B. Banerjee, P. Mondal, A. Bhaumik, and S. M. Islam (2014). *Appl. Catal. A* **469**, 320.

16. M. M. Heravi, E. Hashemi, Y. S. Beheshtiha, S. Ahmadi, and T. Hosseinijad (2014). *J. Mol. Catal. A* **394**, 74.
17. W. R. Reynolds, P. Plucinski, and C. G. Frost (2014). *Catal. Sci. Technol.* **4**, 948.
18. B. D. Briggs, R. T. Pekarek, and M. R. Knecht (2014). *J. Phys. Chem. C* **118**, 18543.
19. B. J. Borah, S. J. Borah, K. Saikia, and D. K. Dutta (2014). *Appl. Catal. A* **469**, 350.
20. A. Alizadeh, M. M. Khodaei, D. Kordestania, and M. Beygzadeh (2013). *J. Mol. Catal. A* **372**, 167.
21. W. Tang, A. G. Capacci, X. Wei, W. Li, A. White, N. D. Patel, J. Savoie, J. J. Gao, S. Rodriguez, B. Qu, N. Haddad, B. Z. Lu, D. Krishnamurthy, N. K. Yee, and C. H. Senanayake (2010). *Angew. Chem.* **122**, 6015.
22. D.-H. Lee and M.-J. Jin (2010). *Org. Lett.* **13**, 252.
23. J.-H. Noh and R. Meijboom (2014). *J. Colloid Interface Sci.* **415**, 57.
24. I. P. Beletskaya and A. V. Cheprakov (2000). *Chem. Rev.* **100**, 3009.
25. A. H. M. de Vries, J. M. C. A. Mulders, J. H. M. Mommers, H. J. W. Henderickx, and J. G. de Vries (2003). *Org. Lett.* **5**, 3285.
26. K. Köhler, R. G. Heidenreich, J. G. E. Krauter, and J. Pietsch (2002). *Chem. A Eur. J.* **8**, 622.
27. V. Polshettiwar and Á. Molnár (2007). *Tetrahedron* **63**, 6949.
28. C. Rossy, J. Majimel, M. T. Delapierre, E. Fouquet, and F.-X. Felpin (2014). *Appl. Catal. A* **482**, 157.
29. M. Nasrollahzadeh, M. Maham, and M. M. Tohidi (2014). *J. Mol. Catal. A* **391**, 83.
30. R. Franzén (2000). *Can. J. Chem.* **78**, 957.
31. J. M. Davidson, C. Triggs (1968). *J. Chem. Soc. A*. 1324–1330.
32. K. Garves (1970). *J. Org. Chem.* **35**, 3273.
33. G. Altenhoff, R. Goddard, C. W. Lehmann, and F. Glorius (2003). *Angew. Chem. Int. Ed.* **42**, 3690.
34. W. A. Herrmann, K. Ófele, S. K. Schneider, E. Herdtweck, and S. D. Hoffmann (2006). *Angew. Chem. Int. Ed.* **45**, 3859.
35. M. Thimmaiah and S. Fang (2007). *Tetrahedron* **63**, 6879.
36. D. J. M. Snelders, G. van Koten, and R. J. M. Klein (2009). Gebbink. *J. Am. Chem. Soc.* **131**, 11407.
37. Y. Uozumi, Y. Matsuura, T. Arakawa, and Y. M. A. Yamada (2009). *Angew. Chem. Int. Ed.* **48**, 2708.
38. M. Lysén and K. Köhler (2005). *Synlett* **2005**, 1671.
39. M. Lysén and K. Köhler (2006). *Synthesis* **2006**, 692.
40. N. Gürbüz, I. Özdemir, T. Seçkin, and B. Çetinkaya (2004). *J. Inorg. Organomet. Polym.* **14**, 149.
41. D. Zhao, Q. Huo, J. Feng, B. F. Chmelka, and G. D. Stucky (1998). *J. Am. Chem. Soc.* **120**, 6024.
42. D. Zhao, J. Sun, Q. Li, and G. D. Stucky (2000). *Chem. Mater.* **12**, 275.
43. E. Vunain, R. Malgas-Enus, K. Jalama, and R. Meijboom (2013). *J. Sol-Gel Sci. Technol.* **68**, 270.
44. R. W. J. Scott, H. Ye, R. R. Henriquez, and R. M. Crooks (2003). *Chem. Mater.* **15**, 3873.
45. I. Yuranov, L. Kiwi-Minsker, P. Buffat, and A. Renken (2004). *Chem. Mater.* **16**, 760.
46. IUPAC (1985). *Pure Appl. Chem.* **57**, 603.
47. N. Ivashchenko, V. Tertykh, V. Yanishpolskii, S. Khainakov, and A. Dikhtiarenko (2011). *Materi- alwiss. Werkstofftech.* **42**, 64.
48. Y. Jiang and Q. Gao (2005). *J. Am. Chem. Soc.* **128**, 716.
49. S. Jana, S. Haldar, and S. Koner (2009). *Tetrahedron Lett.* **50**, 4820.
50. S. Bhunia, R. Sen, and S. Koner (2010). *Inorg. Chim. Acta* **363**, 3993.
51. J. Guerra and M. A. Herrero (2010). *Nanoscale* **2**, 1390.
52. N. T. S. Phan, M. Van Der Sluys, and C. W. Jones (2006). *Adv. Synth. Catal.* **348**, 609.